Locating and Editing Factual Associations in Mamba

Arnab Sen Sharma[*], **David Atkinson**, and **David Bau**
Khoury College of Computer Sciences, Northeastern University

Abstract

We investigate the mechanisms of factual recall in the Mamba state space model. Our work is inspired by previous findings in autoregressive transformer language models suggesting that their knowledge recall is localized to particular modules at specific token locations; we therefore ask whether factual recall in Mamba can be similarly localized. To investigate this, we conduct four lines of experiments on Mamba. First, we apply causal tracing or interchange interventions to localize key components inside Mamba that are responsible for recalling facts, revealing that specific components within middle layers show strong causal effects at the last token of the subject, while the causal effect of intervening on later layers is most pronounced at the last token of the prompt, matching previous findings on autoregressive transformers. Second, we show that rank-one model editing methods can successfully insert facts at specific locations, again resembling findings on transformer LMs. Finally we adapt attention-knockout techniques to Mamba in order to dissect information flow during factual recall. We compare Mamba directly to a similar-sized autoregressive transformer LM and conclude that despite significant differences in architectures, when it comes to factual recall, the two architectures share many similarities.

1 Introduction

Studies of autoregressive transformer language models' (LMs) processing of factual statements such as *The Eiffel Tower is located in Paris* have identified a localized pattern of internal computations when recalling facts (Meng et al., 2022a;b; Geva et al., 2023; Hernandez et al., 2023; Nanda et al., 2023), and have further found that those LMs can be edited by making single-layer rank-one changes in model parameters to alter a specific fact. Although these localized phenomena appear to generalize across autoregressive transformer LMs, the extent to which similar locality might appear in very different architectures—such as recurrent networks (RNNs)—has not yet been investigated.

In this paper we investigate the internal mechanisms of Mamba (Gu & Dao, 2023), a recently-proposed state-space language model, a type of RNN that achieves per-parameter performance that is competitive with transformers. Specifically, we ask whether factual recall within Mamba exhibits locality similar to the patterns observed in autoregressive transformer language models.

Our paper is a case study confronting a key methodological challenge that broadly faces interpretability researchers: as state-of-the-art neural network architectures evolve, we must ask, can the detailed analytical methods and tools developed for one neural architecture, such as transformer LMs, be generalized and applied to a different neural architecture, such as Mamba? In this paper we are able to answer the question with a qualified "yes": we find that many of the methods used to analyze transformers can also provide insights on Mamba. We also discuss mismatches—that is, interpretation methods (such as attention-knockout) that do not transfer to Mamba as easily due to architectural constraints.

We begin by studying whether activation patching (Wang et al., 2022) can be successfully applied to Mamba. Known variously as causal mediation analysis (Vig et al., 2020), causal

[*]Correspondence to sensharma.a@northeastern.edu, Code available at `romba.baulab.info`

tracing (Meng et al., 2022a), and interchange interventions (Geiger et al., 2021), activation patching techniques can successfully identify specific model components in transformer LMs that play crucial roles in performing a task. We ask whether Mamba can be productively studied the same way, even though the architectural components of Mamba are very different: for example, instead of attention heads and MLP modules, Mamba is composed of convolutions, gates, and state-space modules. To answer, we adapt activation patching to Mamba, and ask if any sparsity patterns emerge which provide insights into the respective roles of its components.

We also study whether rank-one model editing can be applied to Mamba. While studies of transformers (Meng et al., 2022a;b; Hase et al., 2024) have found that there are a range of MLP modules within which factual knowledge can be inserted by making a single rank-one change in parameters, Mamba does not have MLP modules, so we ask if there are any other modules that can be similarly edited to insert knowledge. As with previous studies of transformers, the key question is whether factual associations can be edited with both specificity (without interfering with unrelated facts) and generalization (while remaining robust to rewordings of the edited fact).

Finally, we apply methods for understanding the overall information flows in Mamba. Inspired by Geva et al. (2023), we adapt attention-blocking methods to the attention-free Mamba LMs.

In this work we conduct our experiments on Mamba-2.8b, the largest available LM in Mamba family, and for comparison we conduct the same experiments on the similarly sized Pythia-2.8b (Biderman et al., 2023) autoregressive transformer LM.

2 Background on Mamba

Mamba, introduced in Gu & Dao (2023), is a recent family of language models based on state space models (SSMs). SSMs are designed to model the evolution of a hidden state across time with a first-order differential equation (Koopman et al., 1999; Durbin & Koopman, 2012); when they are used as the recurrent state of an RNN, they can enable highly efficient parallelized training (Gu et al., 2021). To achieve good performance in language modeling, the Mamba SSM introduces input-dependent parameterization or *selective*-SSM instead of the traditional time-invariant SSMs. Mamba uses a special architecture called **MambaBlock**[1], which is stacked homogeneously, replacing both attention and MLP blocks used in transformer layers. Here, we focus on the different operations performed inside a MambaBlock.

Formally, Mamba is an autoregressive language model: $M : \mathcal{X} \to \mathcal{Y}$ over a vocabulary $\mathcal{V}$ that maps a sequence of tokens $x = [x_1, x_2, \ldots, x_T] \in \mathcal{X}$, $x_i \in \mathcal{V}$ to $y \in \mathcal{Y} \subset \mathbb{R}^{|\mathcal{V}|}$ which is a probability distribution over the next token continuations of x. Similar to other deep LMs, in Mamba, a token x_i is first embedded to a hidden state of size d as $h_i^{(0)} = emb(x_i)$. Then $h_i^{(0)}$ is transformed sequentially by a series of MambaBlocks. The hidden state $h_i^{(\ell)}$ after the ℓ^{th} (1-indexed) MambaBlock is computed as follows:

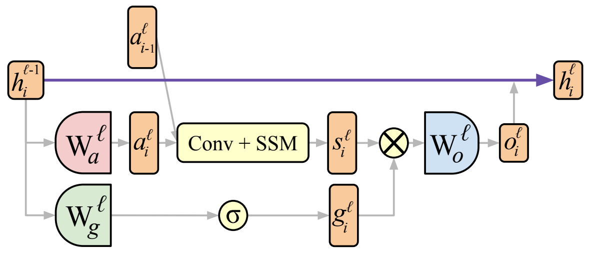

Figure 1: Architecture of a MambaBlock. Projection matrices W_a^{ℓ} and W_g^{ℓ} have the shape $2d \times d$, while W_o^{ℓ} has the shape $d \times 2d$. $h, a, g, s,$ and o are intermediate states of a token representation. σ is SiLU activation and $\otimes$ is elementwise multiplication. *Conv + SSM* operation abstracts the Conv1D and *selective*-SSM operations.

$$h_i^{(\ell)} = h_i^{(\ell-1)} + o_i^{(\ell)} \tag{1}$$

where $o_i^{(\ell)}$ is the output of ℓ^{th} MambaBlock for the i^{th} token

[1]In their paper, Gu & Dao (2023) call this component Mamba—the same name as the LM family.

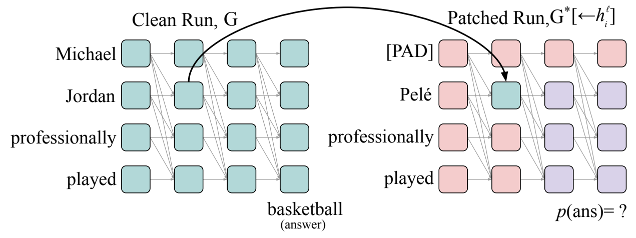

(a) Activation patching

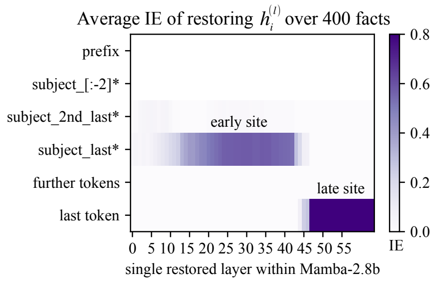

(b) Tracing the residual states, $h_i^{(l)}$

Figure 2: **(a)** Activation patching. A state from the clean run G is *patched* into its corresponding position in the corrupted run G^*. This has a downstream effect of potentially changing all the states that depend on the patched state in $G^*[\leftarrow h_i^{(\ell)}]$. **(b)** Average IE of applying causal tracing on residual stream states $\left(h_i^{(\ell)}\right.$ in Figure 1$\left.\right)$ across 400 different facts from the RELATIONS dataset (See Appendix A.2).

$$o_i^{(\ell)} = \text{MambaBlock}^{(\ell)}\left(h_1^{(\ell-1)}, h_2^{(\ell-1)}, \ldots, h_i^{(\ell-1)}\right) = \text{W}_o^{(\ell)}\left(s_i^{(\ell)} \otimes g_i^{(\ell)}\right) \tag{2}$$

Here, $\otimes$ represents element-wise multiplication or Hadamard product. $s_i^{(\ell)}$ is calculated as:

$$a_i^{(\ell)} = \text{W}_a^{(\ell)} h_i^{(\ell)} \tag{3}$$

$$c_1^{(\ell)}, c_2^{(\ell)}, \ldots, c_i^{(\ell)} = \text{SiLU}\left(\text{Conv1D}\left(a_1^{(\ell)}, a_2^{(\ell)}, \ldots, a_i^{(\ell)}\right)\right) \tag{4}$$

$$s_i^{(\ell)} = \textit{selective}\text{-SSM}\left(c_1^{(\ell)}, c_2^{(\ell)}, \ldots, c_i^{(\ell)}\right) \tag{5}$$

We abstract the operations in Equations 4 and 5 as the **Conv + SSM** operation in Figure 1. At a high level, Conv + SSM brings information from the past token representations to the current token representation, similar to the *attention* blocks in transformer LMs. But, unlike attention operation, Conv + SSM scales *linearly* with the context length and thereby enjoys faster inference speed and longer context limits. See Gu & Dao (2023) for details.

The output of the other path $g_i^{(\ell)}$ (that does not pass through Conv + SSM operation) is a gating mechanism that regulates the information flow. This gating mechanism resembles parts of LSTM (Hochreiter & Schmidhuber, 1997) and GRU (Cho et al., 2014) networks, where similar gates control selective updates of recurrent state.

$$g_i^{(\ell)} = \text{SiLU}\left(\text{W}_g^{(\ell)} h_i^{(\ell-1)}\right) \tag{6}$$

In the remainder of the paper, we aim to characterize the role of the components of Mamba in factual recall by adapting tools that have previously been used to analyze transformers. In Section 3, we apply activation patching to localize factual recall as in Meng et al. (2022a), testing the roles of states s_i, g_i, and o_i at all layers. In Section 4, following Meng et al. (2022a); Hase et al. (2024), we test rank-one edits of facts across components W_a, W_g, and W_o at each layer. And in Section 5 we address the challenge of applying attention patching in Mamba, as used in Geva et al. (2023) to isolate information flow in GPT LMs. We include a further investigation of Mamba's factual recall mechanisms in Appendix E, following Hernandez et al. (2023) in collecting Jacobians within Mamba to test the linearity of its relational encodings.

3 Locating Key States for Factual Recall

We begin with activation patching, seeking to understand if there are specific hidden states which play important roles during factual recall. We select a fact (s, r, o) that the LM knows, where r is a relation that associates a subject entity s with an object entity o. To estimate each state's contribution towards a correct factual prediction (s = *Michael Jordan*, r = *professionally played*, o = *basketball*), we collect model activations across three different runs:

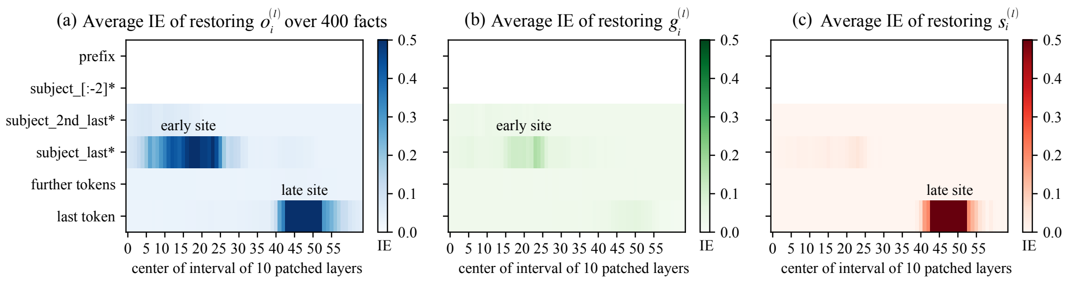

Figure 3: Average indirect effect of different states $o_i^{(\ell)}$, $g_i^{(\ell)}$, and $s_i^{(\ell)}$ over 400 facts from the RELATIONS dataset (see Appendix A.2). For each layer ℓ, states for a window of 10 layers around ℓ are restored from the clean run G.

clean run G: In the clean run, we run the model on a prompt specifying the fact we are interested in. For example, $x = (s, r) =$ *Michael Jordan professionally played*. We cache all the hidden states during the clean run to be used later: $\{h_i^{(\ell)}, a_i^{(\ell)}, s_i^{(\ell)}, g_i^{(\ell)} \mid i \in [1, T],\ \ell \in [1, L]\}$.

corrupted run G^*: In the corrupted run, we swap s with a different subject s^* (*Pelé*) such that the LM gives a different answer o^* (*soccer*) to the modified prompt $x^* = (s^*, r)$ (i.e., $o^* \neq o$).

This subject-swapping approach follows the recommendation of Zhang & Nanda (2023) and has the advantage of using natural text perturbations to avoid introducing out-of-domain states to the model's computation, as may happen when corrupting s embeddings with Gaussian noise (the method used in Meng et al. (2022a)).

patched run $G^*[\leftarrow h_i^{(\ell)}]$: In the patched run, we run the model on the corrupted prompt x^*, but intervene on $h_i^{(\ell)}$ by replacing its value with the corresponding state cached from the clean run G. The remainder of the computation is run normally, meaning that the patched state can have a downstream effect of potentially changing all the states that depend on it. See Figure 2a.

Let $p(o)$, $p^*(o)$, and $p^*[\leftarrow h_i^{(\ell)}](o)$ denote the probability assigned to the correct answer o in G, G^*, and $G^*[\leftarrow h_i^{(\ell)}]$ respectively. To measure the contribution of $h_i^{(\ell)}$ in recalling the fact (s, r, o), we define its *indirect effect* (IE) as:

$$\mathrm{IE}_{h_i^{(\ell)}} = \frac{p^*[\leftarrow h_i^{(\ell)}](o) - p^*(o)}{p(o) - p^*(o)} \tag{7}$$

In Figure 2b we plot the average indirect effect of restoring the residual states $h_i^{(\ell)}$ across different layer-token positions over 400 facts from the RELATIONS dataset (Hernandez et al., 2023). The high IE observed at the *late site* (later layers at the last token) position is natural, as restoring a clean $h_i^{(\ell)}$ there will restore most of the model computation from G. However, Mamba also shows high causality at the *early site* (early-middle layers at the last subject token position). This is consistent with what Meng et al. (2022a) observed in GPT LMs.

In Figure 3 we plot the average IE for $o_i^{(\ell)}$, $g_i^{(\ell)}$, and $s_i^{(\ell)}$. The plot for $o_i^{(\ell)}$ (Figure 3a) looks very similar to Figure 2b, confirming that the output from MambaBlock has strong causal effects at both early and late sites. Interestingly, Figure 3c shows that the selective-SSM outputs $s_i^{(\ell)}$ have high IE only at the late site, resembling the behavior of attention modules in GPT models (Meng et al., 2022a). However, there is no state that appears to do the opposite; in other words, there is no state with strong effects at the early site and not at the late site (The gate output $g_i^{(\ell)}$ does have stronger IE at the early site, but these effects are very weak). To compare with autoregressive transformer LMs, activation patching results for Pythia-2.8b is shown in Figure 9 in Appendix D. This comparison reveals a key way how Mamba differs from transformers: while transformer MLP outputs have effects in the early

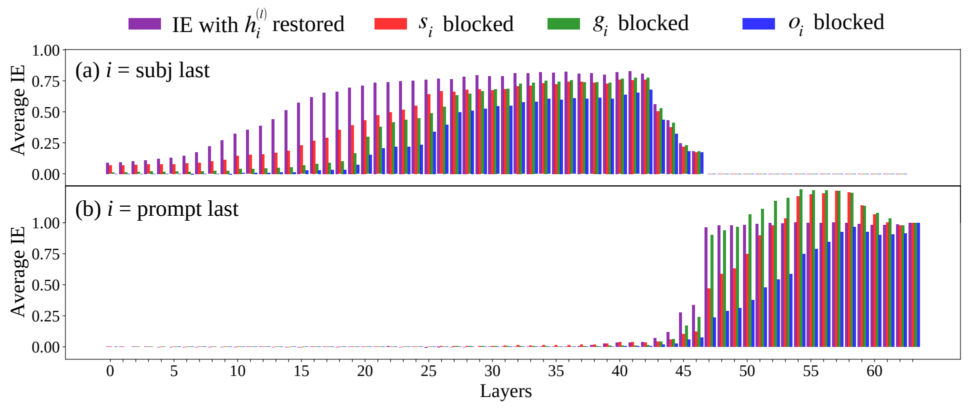

Figure 5: Impact of ablating s_i, g_i, and o_i on $\text{IE}_{h_i^{(\ell)}}$ for **(a)** *subject last* and **(b)** *prompt last* token positions. Taken together (a) and (b) show a clear separation roles between early-mid and later layers in Mamba-2.8b. $h_i^{(\ell)}$ up to layer 46 only show strong IE at the subject last token position and have negligible impact after that. Whereas IE of $h_i^{(\ell)}$ jumps to 1.0 after layer 46. **(a)** also shows that, at the subject last token, before layer $27-28$, $\text{IE}_{h_i^{(\ell)}}$ is significantly reduced by blocking either o_i, g_i, or s_i paths (sorted in descending order of damaging $\text{IE}_{h_i^{(\ell)}}$). **(b)** At the prompt last token, ablating o_i or s_i paths can significantly reduce $\text{IE}_{h_i^{(\ell)}}$ in layers $47-50$.

site and not the late site, in Mamba there is no similar state that specializes only at the early site, at which factual recall would be expected to occur. This presents the question: which parameters in Mamba mediate factual recall?

To investigate this question, we replicate an experiment from Meng et al. (2022a) to probe *path-specific effects* (Pearl, 2022) by severing a path from the causal graph and monitoring its effect. Here, we are interested in understanding the effect of the contributions from g_i, s_i, and o_i (i.e. states that are processed by W_g, Conv + SSM, and W_o respectively) while recalling a fact. First, in the corrupted run G^*, at token position i, we cache all the contributions from the s_i paths as $s_i^* = \{s_i^{*(\ell)} | \ \ell \in [1, L]\}$. Then in the patched run $G^*[\leftarrow h_i^{(\ell)}]$, we restore $h_i^{(\ell)}$ that was cached from the clean run G into its corresponding state (as in Figure 2a), but with an additional modification: to understand the contribution from the s_i paths, we sever those paths by also patching s_i^* (cached from the corrupted run G^*) to their corresponding locations (see Figure 4). The same experiment is replicated to understand the contributions of g_i and o_i states. We note that severing the $o_i^{(\ell)}$ will sever $s_i^{(\ell)}$ and $g_i^{(\ell)}$ as well (see Figure 1).

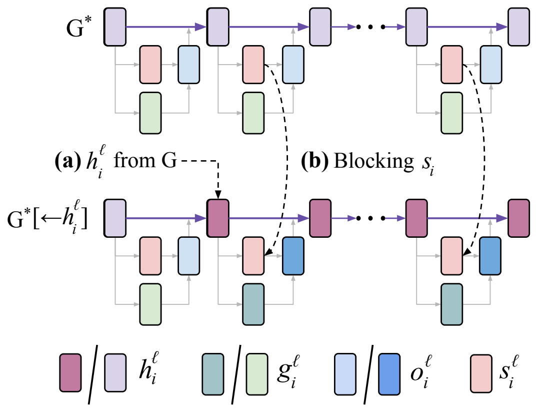

Figure 4: To probe for path-specific effects, **(a)** $h_i^{(\ell)}$ is restored from the clean run G (as in Figure 2a). **(b)** Then, to reveal the role of the Conv + SSM contributions, s_i^* states from the corrupted run G^* are also patched to block the contributions from s_i paths.

In Figure 5 we plot the average results of this experiment for token positions (a) $i =$ *subject last* and (b) $i =$ *prompt last* over 400 examples randomly sampled from the RELATIONS dataset. The key findings can be understood by examining the gap between the purple bars and the red, green, and blue bars: a large gap indicates a strong mediating role for Conv + SSM, W_g, or W_o parameters, respectively. At the early site at the subject last token, both the Conv + SSM and W_g have a strong role, but W_o plays an even larger role than either. Yet the strongest mediator at the late site is also W_o. This experiment highlights the importance of W_o in both stages of predicting a fact. But it also suggests that Mamba does not separate early-site factual recall between these groups of parameters as cleanly as transformers. However, Figure 5 reveals a clean separation of roles between early to mid and later layers, analogous to the findings of Hernandez et al. (2023) in transformer LMs. We also note that this division of responsibilities between layers can be more sharply noticed in Mamba when compared to transformers LMs (compare Figure 5 with Figure 10).

4 Editing Facts With ROME

Having begun to characterize the locations of important states for factual recall, we now investigate whether factual recall behavior can be edited. In particular, we apply the ROME (Rank One Model Editing, Meng et al., 2022a) technique to Mamba. ROME begins with the observation that any linear transformation can be considered as an associative memory (Anderson, 1972; Kohonen, 1972), mapping a set of keys $K = [k_1|k_2|\dots]$ to their corresponding values $V = [v_1|v_2|\dots]$, and uses this to edit factual associations in transformer LMs. Here, we apply the technique to a particular set of linear transformations within Mamba, and report our editing success on each.[2]

The input to ROME is a prompt $x = (s, r)$, where s (*Emmanuel Macron*) is a subject entity and r (*is the President of*) is a relation. ROME also takes a counterfactual object o^* (*England*), meant to replace the correct object o (*France*) in the model's output. To effect that change, ROME generates a rank-one update to $\mathrm{W}_{down}^{(\ell)}$, the down-projection matrix of the MLP module for the last token of the subject at layer ℓ—which plays the role of the associative memory. In generating the rank-one update, ROME considers the input to $\mathrm{W}_{down}^{(\ell)}$ as the *key* (k_*). Then, with gradient descent ROME calculates a *value* (v_*) such that, when v_* is inserted as the output of $\mathrm{W}_{down}^{(\ell)}$, the model will output o^*. Importantly, while optimizing v_*, ROME attempts to minimize unrelated changes in model outputs (*Joe Biden*, for example, should still be mapped to *the United States* post-edit). Finally, ROME adds a rank-1 matrix Δ to $\mathrm{W}_{down}^{(\ell)}$ such that $\left(\mathrm{W}_{down}^{(\ell)} + \Delta\right)k_* \approx v_*$. (See Meng et al. (2022a) for details.)

4.1 Applying ROME in Mamba

We apply ROME on the three different projection matrices of Mamba: $\mathrm{W}_a^{(\ell)}$ which affects only the Conv + SSM path, $\mathrm{W}_g^{(\ell)}$ which affects only the gating path, and $\mathrm{W}_o^{(\ell)}$, the final output of the MambaBlock, which is added to the residual state. We plot ROME performance on different projection matrices $\left(\mathrm{W}_a^{(\ell)}, \mathrm{W}_g^{(\ell)}, \text{and } \mathrm{W}_o^{(\ell)}\right)$ across all the layers in Figure 6a.

To evaluate editing performance, we use the CounterFact dataset from Meng et al. (2022a). CounterFact contains 20K counterfactual examples in the form $(s, r, o \to o^*)$, where o is the correct answer to the prompt $x = (s, r)$, and o^* is the object which is to be inserted as the new answer to the prompt (See Appendix A.1 for details). We select the first 2000 examples from this dataset for our module-layer sweep. We use the original evaluation matrices in Meng et al. (2022a) to measure ROME edit performance. The final **score (S)** in the ROME evaluation suite is the harmonic mean of three different scores:

1. **Efficacy (ES)**: For an edit request $(s, r, o \to o^*)$, we say the edit is *effective* if, post-edit, the LM assigns $p(o^*) > p(o)$ in response to the prompt $x = (s, r)$. Efficacy reflects the portion of the examples where the edit was effective.
2. **Generalization (PS)**: A successful edit should be persistent across different paraphrases of (s, r). For each of the request instances $(s, r, o \to o^*)$, $p(o^*) > p(o)$ is checked post-edit with a set of different rephrasings $x_p \sim \mathcal{P}_r(s)$ of the prompt $x = (s, r)$, where $\mathcal{P}_r$ denotes a set of paraphrased templates for the relation r.

[2]Further motivating these experiments, previous work has shown that the locations identified by activation patching techniques are not necessarily those which have the strongest edit performance (Hase et al., 2024).

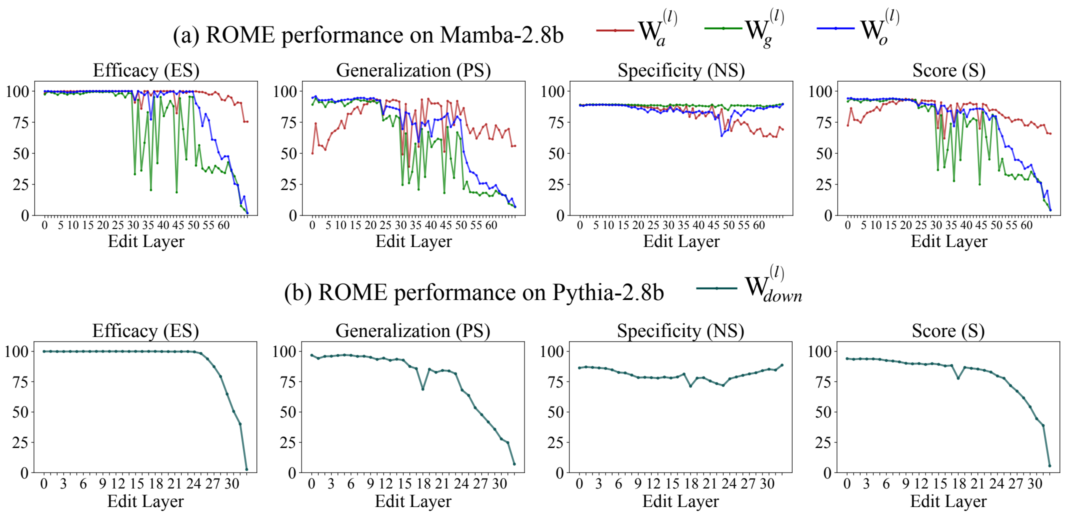

Figure 6: ROME performance in editing facts across different layers **(a)** by modifying $W_a^{(\ell)}$, $W_g^{(\ell)}$, $W_o^{(\ell)}$ in Mamba-2.8b, and **(b)** modifying $W_{down}^{(\ell)}$ in Pythia-2.8b. Results are reported on the first 2000 examples in the COUNTERFACT dataset.

3. **Specificity (NS)**: Finally, the edit should be specific to $\mathcal{P}_r(s)$ and should not additionally change the mapping of some nearby subject s_n to o^*. To evaluate the specificity of an edit we measure $p(o_n) > p(o^*)$ with $\mathcal{P}_r(s_n)$ for a set of nearby factual associations $\{(s_n, r, o_n) \mid o_n \neq o^*\}$.

Figure 6a shows that ROME can achieve high scores (S) for a range of early to middle layers by modifying any one of the projection matrices $W_a^{(\ell)}$, $W_g^{(\ell)}$, or $W_o^{(\ell)}$, matching observations made by Hase et al. (2024) regarding transformer LMs. However, we found that performance does depend on the location of the edit. For example, in the case of $W_g^{(\ell)}$ and $W_o^{(\ell)}$, the score (S) and generalization (PS) drops after around layer 43. This is consistent with our findings from the path-blocking experiment in Figure 5a. We also find that edits to $W_a^{(\ell)}$ have poor generalization (PS) in early layers, whereas high PS can be achieved at early layers by modifying either $W_g^{(\ell)}$ or $W_o^{(\ell)}$, consistent with their higher indirect effects as seen in Figure 5a.

Where is the right place to apply ROME on Mamba? Figure 3 could suggest $W_g^{(\ell)}$, since the causal effect of g_i states is mostly concentrated at the subject last token, similar to the behavior of MLPs in transformers (Meng et al., 2022a). Consistent with this is the architectural fact that, just as transformers' $W_{down}^{(\ell)}$ connects to attention modules only through the residual stream, the output of $W_g^{(\ell)}$ does not flow through the Conv + SSM module—a module that other work has suggested might play a role similar to that played by attention heads in transformers (Grazzi et al., 2024). And, indeed, we find that ROME can successfully insert facts by modifying $W_g^{(\ell)}$. On the other hand Figure 6a reveals sudden drops in efficacy and generalization at middle layer gates, suggesting that $W_g^{(\ell)}$ may be an unreliable mediator at some layers. Our experiments further show that the best performance for ROME is empirically achieved by modifying $W_o^{(\ell)}$. This is consistent with the fact that o_i states show a stronger causal effect at the subject last token than g_i states do (see Figures 3a and 5a). Additionally, ROME achieves better generalization (PS), competitive specificity (NS), and an overall better score (S) with $W_o^{(\ell)}$. We hypothesize that the strong performance of $W_o^{(\ell)}$ may be due to the the separation of roles between early-mid and later layers observed in Figures 2b, 3a, and 5. Also see Appendix C where we isolate the contribution of $W_o^{(\ell)}$ by

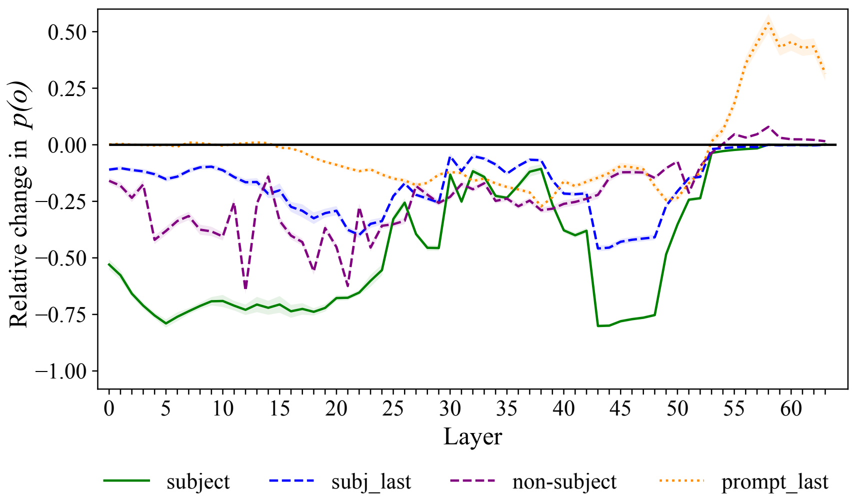

Figure 7: Relative change in $p(o)$ when information flow from $a_k^{(\ell)}$ to future tokens via s_i paths is blocked, with k taking the value of either *subject*, *non-subject*, or the *prompt_last* token positions. For each layer ℓ, s_i paths were blocked for a window of 10 layers around ℓ.

subtracting $\text{IE}_{s_i^{(\ell)}} + \text{IE}_{g_i^{(\ell)}}$ from $\text{IE}_{o_i^{(\ell)}}$, which reveal a critical role of $W_o^{(\ell)}$ in early-mid layers at subject last token position while mediating a fact.

We plot ROME performance for a similar sized Pythia model on Figure 6b for comparison.

5 Attention Knock-out in Mamba?

Attention modules mediate the flow of information across different token positions in transformer LMs. In attention *"knock-out"* experiments the information that flows through a specific edge (from k^{th} token to q^{th} token) via a certain attention head is blocked to understand if critical information flows through that edge. This is also a form of causal mediation analysis and it has been effective in understanding the information flow in transformer LMs (Geva et al., 2023; Wang et al., 2022; Todd et al., 2023). In Mamba, information from past tokens is retained in the s_i states, with the Conv + SSM operations (see Figure 1 and Equations 3–5). We ask, can we perform experiments similar to attention knock-out experiments in Mamba in order to understand how it moves factual information?

We find that performing similar experiments in Mamba can be difficult. The use of Conv with a non-linearity in conjunction with selective-SSM make it challenging to remove the information retained in the q^{th} token from the k^{th} token (see Appendix B for details). However, it is possible to block the propagation of information from the k^{th} token to *all* the future tokens via Conv + SSM with mean-ablation. Specifically, for a layer ℓ, we set $a_k^{(\ell)} := \mathbb{E}\left[a^{(\ell)}\right]$, where $\mathbb{E}\left[a^{(\ell)}\right]$ is the mean of $a^{(\ell)}$ states collected with 10,000 tokens from WikiText-103 by Merity et al. (2016). We recognize that this intervention may not be as *surgical* as cutting a specific edge. However, with some caveats, this experiment suggests that the factual information flow in Mamba is similar to what Geva et al. (2023) observed in GPT LMs.

We randomly sample 700 facts across 6 factual relations from the RELATIONS dataset. For each of those examples we block-out information propagation of the *subject*, *non-subject*, and the *prompt-last* token positions for a window of 10 layers around a specific layer ℓ. The effect of blocking out Conv + SSM information flow for certain layer-token $(\ell - k)$ positions is measured as the relative change in $p(o)$ with $\left(p\left(o \mid a_k^{(\ell)} := \mathbb{E}\left[a^{(\ell)}\right]\right) - p(o)\right)/p(o)$. Figure 7 shows the averaged result and it leads us to draw the following conclusions about how factual information flows in Mamba:

(a) The purple lines show that blocking out non-subject information flow in early middle layers can bring down $p(o)$ by up to 50%. Non-subject tokens are used to specify the relation r. This observation leads us to believe that Mamba propagates relation specific information to future tokens using Conv+SSM operations in early-middle layers.

(b) Interestingly, the green lines (blocking the subject information flow) shows two valleys:

1. The first valley at the early layers is not surprising as Mamba needs to collate information from all the subject tokens in early layers to recognize a subject entity s consisting of multiple tokens.
2. However, the valley at layers 43-48 suggest that Mamba uses Conv + SSM paths in those layers to propagate critical information from the subject to later tokens. This aligns with Figures 5b and 3c, where s_i states in those layers show high indirect effects, indicating their crucial role while recalling a fact.

(c) The blue dashed lines indicate the effect of blocking the information of only the subject last token. If the ablation is performed in very early layers, later layers can start to compensate for that. However, the valley around layers 20-21 suggests that Mamba expects to recognize the full subject entity by then in order to recall relevant associations (*enrichment*). Notably, activation patching results for o_i and s_i—states that we hypothesize take crucial part in the enrichment process—also show strong indirect effect around that region (Figures 3a, 3b, and 5a). The blue line follows the green line after layer 30. The weaker effect observed might be because ablating subject last token is not always enough to remove all the subject information. For example, in *Eiffel Tower*, *Eiffel* (tokenized as `E`, `iff`, `el`) is more informative than the last token `Tower`.

These findings align with how factual information flows through attention modules in autoregressive transformer LMs, as observed by Geva et al. (2023) in GPT. However, unlike Geva et al. (2023), we cannot make strong claims about the unique role of the final token position (prompt-last) with this experiment. As we block out information flow to *all* future tokens, the intermediate states in between the ablated k^{th} token and the last token are affected as well.

6 Related Works

Mamba. Mamba is a recent family of language models that are based on state space models (SSMs). Neural SSM-based models have achieved good performance across different modalities, including vision (Nguyen et al., 2022), audio (Goel et al., 2022), and genomic sequences (Nguyen et al., 2023). Only recently, however, with Mamba, have they become competitive with the language modeling performance of transformers (Gu & Dao, 2023). Like transformers, Mamba contains factual knowledge about real world entities (Grazzi et al., 2024). However, knowledge representation in Mamba (and other LMs based on SSMs) has up to now remained unexplored.

There are few works focused on interpreting Mamba. Ali et al. (2024) identify implicit attention-like matrices formed by Mamba's selective state space layers. Grazzi et al. (2024), while not strictly focused on interpreting Mamba's internals, apply linear probes to Mamba's (decoded) intermediate states during in-context regression tasks. They discover substantial similarities between Mamba and transformer models: both architectures pursue "iterative" strategies, with the task loss falling more or less monotonically as the layer index increases. Finally, in concurrent work, Paulo et al. (2024) apply a different set of interpretability techniques to Mamba, focusing on activation steering and linear probing methods. Like us, they find that approaches developed for transformer models largely transfer to Mamba.

Locating Factual Knowledge in Language Models. To make factually correct statements about the world, a LM has to store factual knowledge about real world entities somewhere in its parameters. Understanding how and where a neural network stores knowledge is a core problem for interpretability and it has thus been studied from several perspectives (Ji et al., 2021; Wang et al., 2014). One line of work trains classifiers to probe for properties encoded in model representations (Ettinger et al., 2016; Shi et al., 2016; Hupkes et al., 2018; Conneau et al., 2018; Belinkov et al., 2017; Belinkov & Glass, 2019). However, the flexibility of these classifiers can lead to overestimating model knowledge and capabilites (Belinkov, 2022). Causal mediation analysis methods (Pearl, 2022) attempt to measure the causal contribution of intermediate states to task performance. Meng et al. (2022a;b) use activation patching to identify key MLP modules for factual recall, highlighting the middle layers at particular token positions as being especially important. Similarly, Geva et al. (2023) apply causal mediation analysis to attention modules, seeking to understand the mechanism of cross-token factual information flow inside transformer LMs.

7 Discussion

In this paper we have set out to understand whether the analytical methods and tools developed for transformer LMs can also be applied on the Mamba LMs based on recurrent state-space architecture. Although our experiments have been limited to Mamba-2.8b, the largest available LM of that family, and comparisons to the similarly-sized transformer Pythia-2.8b, the methods we have investigated are general, and can be used to analyze to any state-space model.

Our overall comparisons of Mamba and transformers are positive: with activation patching we have found that, similar to autoregressive transformer LMs, Mamba shows signs of localization at the last subject token and at specific layer ranges while recalling a fact. Although, unlike transformers, Mamba has no MLP modules, we find that their W_o weights can receive rank-one model editing (ROME) edits with good generalization and specificity at a range of layers, similar to W_{down} in Pythia and GPT family of LMs. We have also been able to partially adapt the tools of attention knock-out in Mamba by blocking outgoing information from a token, revealing information flows similar to transformer LMs during factual recall.

The similarity that we have observed between factual recall mechanisms in transformers and Mamba leads us to speculate that the autoregressive language modeling task itself induces a pattern of localized factual recall that is independent of modeling architecture. When constraining a model to process text from beginning to end, the ordering creates a specific bottleneck in the information flows: the end of a subject becomes a singular moment at which recognition of the subject is both possible and useful, and we find that both transformers and Mamba arrange their computations to localize factual recall at that moment. We hypothesize that other future autoregressive LMs architectures should expect to see similar locality in factual recall as well.

In summary, we find that many of the tools used to interpret and edit large transformers can be adapted to work with Mamba, and we are optimistic that those tools will continue to be useful as architectures contitute to evolve.

Ethics

By exploring the factual recall mechanism in Mamba, we potentially improve its transparency, enabling oversight and control. However, the ability to modify facts directly in the model brings with it the potential for abuse, such as adding malicious misinformation or bias.

Reproducibility

We ran all experiments on workstations with either 80GB NVIDIA A100 GPUs or 48GB A6000 GPUs, using the HuggingFace Transformers library (Wolf et al., 2019) and PyTorch (Paszke et al., 2019). We make use of publicly available datasets COUNTERFACT and RELATIONS in this work.

Acknowledgements

This research has been supported by a grant from Open Philanthropy (DB, AS), and an NSF Computer and Information Science and Engineering Graduate Fellowship Fellowship (DA). We are also grateful to the Center for AI Safety (CAIS) for sharing their compute resources, which supported many of our experiments. Some of our initial analyses were conducted with a beta version of `NNsight` (Fiotto-Kaufman et al., 2024) on an implementation of Mamba instrumented for research by Jaden Fiotto-Kaufmann.

References

Ameen Ali, Itamar Zimerman, and Lior Wolf. The hidden attention of mamba models. *arXiv preprint arXiv:2403.01590*, 2024.

James A Anderson. A simple neural network generating an interactive memory. *Mathematical biosciences*, 14(3-4):197–220, 1972.

Yonatan Belinkov. Probing classifiers: Promises, shortcomings, and advances. *Computational Linguistics*, 48(1):207–219, 2022.

Yonatan Belinkov and James Glass. Analysis methods in neural language processing: A survey. *Transactions of the Association for Computational Linguistics*, 7:49–72, 2019.

Yonatan Belinkov, Nadir Durrani, Fahim Dalvi, Hassan Sajjad, and James Glass. What do neural machine translation models learn about morphology? *arXiv preprint arXiv:1704.03471*, 2017.

Stella Biderman, Hailey Schoelkopf, Quentin Gregory Anthony, Herbie Bradley, Kyle O'Brien, Eric Hallahan, Mohammad Aflah Khan, Shivanshu Purohit, USVSN Sai Prashanth, Edward Raff, et al. Pythia: A suite for analyzing large language models across training and scaling. In *International Conference on Machine Learning*, pp. 2397–2430. PMLR, 2023.

Kyunghyun Cho, Bart Van Merriënboer, Dzmitry Bahdanau, and Yoshua Bengio. On the properties of neural machine translation: Encoder-decoder approaches. *arXiv preprint arXiv:1409.1259*, 2014.

Alexis Conneau, German Kruszewski, Guillaume Lample, Loïc Barrault, and Marco Baroni. What you can cram into a single vector: Probing sentence embeddings for linguistic properties. *arXiv preprint arXiv:1805.01070*, 2018.

James Durbin and Siem Jan Koopman. *Time series analysis by state space methods*, volume 38. OUP Oxford, 2012.

Yanai Elazar, Nora Kassner, Shauli Ravfogel, Abhilasha Ravichander, Eduard Hovy, Hinrich Schütze, and Yoav Goldberg. Measuring and improving consistency in pretrained language models. *Transactions of the Association for Computational Linguistics*, 9:1012–1031, 2021.

Allyson Ettinger, Ahmed Elgohary, and Philip Resnik. Probing for semantic evidence of composition by means of simple classification tasks. In *Proceedings of the 1st workshop on evaluating vector-space representations for nlp*, pp. 134–139, 2016.

Jaden Fiotto-Kaufman, Alexander R Loftus, Eric Todd, Jannik Brinkmann, Caden Juang, Koyena Pal, Can Rager, Aaron Mueller, Samuel Marks, Arnab Sen Sharma, et al. Nnsight and ndif: Democratizing access to foundation model internals. *arXiv preprint arXiv:2407.14561*, 2024.

Atticus Geiger, Zhengxuan Wu, Hanson Lu, Josh Rozner, Elisa Kreiss, Thomas Icard, Noah D. Goodman, and Christopher Potts. Inducing causal structure for interpretable neural networks. *CoRR*, abs/2112.00826, 2021. URL https://arxiv.org/abs/2112.00826.

Mor Geva, Jasmijn Bastings, Katja Filippova, and Amir Globerson. Dissecting recall of factual associations in auto-regressive language models. *arXiv preprint arXiv:2304.14767*, 2023.

Karan Goel, Albert Gu, Chris Donahue, and Christopher Re. It's raw! Audio generation with state-space models. In Kamalika Chaudhuri, Stefanie Jegelka, Le Song, Csaba Szepesvari, Gang Niu, and Sivan Sabato (eds.), *Proceedings of the 39th International Conference on Machine Learning*, volume 162 of *Proceedings of Machine Learning Research*, pp. 7616–7633. PMLR, 17–23 Jul 2022. URL https://proceedings.mlr.press/v162/goel22a.html.

Riccardo Grazzi, Julien Siems, Simon Schrodi, Thomas Brox, and Frank Hutter. Is Mamba Capable of In-Context Learning?, 2024. URL http://arxiv.org/abs/2402.03170.

Albert Gu and Tri Dao. Mamba: Linear-time sequence modeling with selective state spaces. *arXiv preprint arXiv:2312.00752*, 2023.

Albert Gu, Karan Goel, and Christopher Ré. Efficiently modeling long sequences with structured state spaces. *arXiv preprint arXiv:2111.00396*, 2021.

Peter Hase, Mohit Bansal, Been Kim, and Asma Ghandeharioun. Does localization inform editing? surprising differences in causality-based localization vs. knowledge editing in language models. *Advances in Neural Information Processing Systems*, 36, 2024.

Evan Hernandez, Arnab Sen Sharma, Tal Haklay, Kevin Meng, Martin Wattenberg, Jacob Andreas, Yonatan Belinkov, and David Bau. Linearity of relation decoding in transformer language models. *arXiv preprint arXiv:2308.09124*, 2023.

Sepp Hochreiter and Jürgen Schmidhuber. Long short-term memory. *Neural computation*, 9 (8):1735–1780, 1997.

Dieuwke Hupkes, Sara Veldhoen, and Willem Zuidema. Visualisation and'diagnostic classifiers' reveal how recurrent and recursive neural networks process hierarchical structure. *Journal of Artificial Intelligence Research*, 61:907–926, 2018.

Shaoxiong Ji, Shirui Pan, Erik Cambria, Pekka Marttinen, and S Yu Philip. A survey on knowledge graphs: Representation, acquisition, and applications. *IEEE Transactions on Neural Networks and Learning Systems*, 33(2):494–514, 2021.

Teuvo Kohonen. Correlation matrix memories. *IEEE transactions on computers*, 100(4): 353–359, 1972.

Siem Jan Koopman, Neil Shephard, and Jurgen A Doornik. Statistical algorithms for models in state space using ssfpack 2.2. *The Econometrics Journal*, 2(1):107–160, 1999.

Kevin Meng, David Bau, Alex Andonian, and Yonatan Belinkov. Locating and editing factual associations in gpt. *Advances in Neural Information Processing Systems*, 35:17359–17372, 2022a.

Kevin Meng, Arnab Sen Sharma, Alex Andonian, Yonatan Belinkov, and David Bau. Mass-editing memory in a transformer. *arXiv preprint arXiv:2210.07229*, 2022b.

Stephen Merity, Caiming Xiong, James Bradbury, and Richard Socher. Pointer sentinel mixture models. *arXiv preprint arXiv:1609.07843*, 2016.

Neel Nanda, Senthooran Rajamanoharan, János Kramár, and Rohin Shah. Fact finding: Attempting to reverse-engineer factual recall on the neuron level, 2023. URL https://www.lesswrong.com/posts/iGuwZTHWb6DFY3sKB/fact-finding-attempting-to-reverse-engineer-factual-recall.

Eric Nguyen, Karan Goel, Albert Gu, Gordon Downs, Preey Shah, Tri Dao, Stephen Baccus, and Christopher Ré. S4nd: Modeling images and videos as multidimensional signals with state spaces. In S. Koyejo, S. Mohamed, A. Agarwal, D. Belgrave, K. Cho, and A. Oh (eds.), *Advances in Neural Information Processing Systems*, volume 35, pp. 2846–2861. Curran Associates, Inc., 2022. URL https://proceedings.neurips.cc/paper_files/paper/2022/file/13388efc819c09564c66ab2dc8463809-Paper-Conference.pdf.

Eric Nguyen, Michael Poli, Marjan Faizi, Armin Thomas, Callum Birch-Sykes, Michael Wornow, Aman Patel, Clayton Rabideau, Stefano Massaroli, Yoshua Bengio, Stefano Ermon, Stephen A. Baccus, and Chris Ré. Hyenadna: Long-range genomic sequence modeling at single nucleotide resolution, 2023.

Adam Paszke, Sam Gross, Francisco Massa, Adam Lerer, James Bradbury, Gregory Chanan, Trevor Killeen, Zeming Lin, Natalia Gimelshein, Luca Antiga, et al. Pytorch: An imperative style, high-performance deep learning library. *Advances in neural information processing systems*, 32, 2019.

Gonçalo Paulo, Thomas Marshall, and Nora Belrose. Does transformer interpretability transfer to rnns? *arXiv preprint arXiv:2404.05971*, 2024. URL https://arxiv.org/abs/2404.05971.

Judea Pearl. Direct and indirect effects. In *Probabilistic and causal inference: the works of Judea Pearl*, pp. 373–392. 2022.

Xing Shi, Inkit Padhi, and Kevin Knight. Does string-based neural mt learn source syntax? In *Proceedings of the 2016 conference on empirical methods in natural language processing*, pp. 1526–1534, 2016.

Eric Todd, Millicent L Li, Arnab Sen Sharma, Aaron Mueller, Byron C Wallace, and David Bau. Function vectors in large language models. *arXiv preprint arXiv:2310.15213*, 2023.

Ashish Vaswani, Noam Shazeer, Niki Parmar, Jakob Uszkoreit, Llion Jones, Aidan N Gomez, Łukasz Kaiser, and Illia Polosukhin. Attention is all you need. *Advances in neural information processing systems*, 30, 2017.

Jesse Vig, Sebastian Gehrmann, Yonatan Belinkov, Sharon Qian, Daniel Nevo, Yaron Singer, and Stuart Shieber. Investigating gender bias in language models using causal mediation analysis. In H. Larochelle, M. Ranzato, R. Hadsell, M.F. Balcan, and H. Lin (eds.), *Advances in Neural Information Processing Systems*, volume 33, pp. 12388–12401. Curran Associates, Inc., 2020. URL https://proceedings.neurips.cc/paper_files/paper/2020/file/92650b2e92217715fe312e6fa7b90d82-Paper.pdf.

Kevin Wang, Alexandre Variengien, Arthur Conmy, Buck Shlegeris, and Jacob Steinhardt. Interpretability in the wild: a circuit for indirect object identification in gpt-2 small. *arXiv preprint arXiv:2211.00593*, 2022.

Zhen Wang, Jianwen Zhang, Jianlin Feng, and Zheng Chen. Knowledge graph embedding by translating on hyperplanes. In *Proceedings of the AAAI conference on artificial intelligence*, volume 28, 2014.

Thomas Wolf, Lysandre Debut, Victor Sanh, Julien Chaumond, Clement Delangue, Anthony Moi, Pierric Cistac, Tim Rault, Rémi Louf, Morgan Funtowicz, et al. Huggingface's transformers: State-of-the-art natural language processing. *arXiv preprint arXiv:1910.03771*, 2019.

Fred Zhang and Neel Nanda. Towards best practices of activation patching in language models: Metrics and methods. *arXiv preprint arXiv:2309.16042*, 2023.

A Datasets

We use two datasets; CounterFact by Meng et al. (2022a) and Relations by Hernandez et al. (2023) in this work.

A.1 CounterFact

Meng et al. (2022a) developed the CounterFact dataset for evaluating the efficacy of counterfactual edits in language models. It was prepared by adapting ParaRel (Elazar et al. (2021)) and scraping *Wikidata*[3]. The dataset contains 21,919 requests $\{s, r, o, o^*, \pi^*\}$ where o is the correct answer to the prompt $x = (s, r)$, o^* is the counterfactual edit request, and $\pi^* \sim \mathcal{P}(s, r)$ is a paraphrase of the prompt $x = (s, r)$ to test for generalizability (PS). Each of the records also contain some neighborhood prompts π_N to test for specificity (NS) and some generation prompts π_G to test if LM generation post-edit is fluent and consistent with the edit. Please refer to Meng et al. (2022a) for details on the curation of this dataset.

We evaluate ROME performance in Mamba-2.8b (Figure 6a) and Pythia-2.8b (Figure 6b) on the first 2000 records from CounterFact.

A.2 Relations

The Relations dataset introduced in Hernandez et al. (2023) consists of 47 relations of 4 types: *factual*, *linguistic*, *bias*, and *commonsense*. A relation r is an association between two entities. For example, the relation, $r =$ *professionally played the sport* connects the subject $s =$ *Michael Jordan* with the object $o =$ *basketball*. The dataset contains a set of (s, o) for each relation r.

In the scope of this paper, we only utilize the 26 *factual* relations from this dataset. We evaluate Lre in Mamba and Pythia for all the 26 factual relations. We also use this dataset for locating key fact-mediating states in Section 3 and Appendix D. We randomly sample 400 examples (s, r, o) across 6 different factual relations - *place in city*, *country capital city*, *person occupation*, *plays pro sport*, *company hq*, and *product by company*. For each of these examples we randomly select another example within the same relation (s^*, r, o^*) such that $s \neq s^*$ and $o \neq o^*$. The average indirect effect (IE) of applying activation patching over these 400 examples is depicted on Figures 2b, 3, 5 for Mamba-2.8b) and on Figure 9 (for Pythia-2.8b). We use the same set of 6 relations in Section 5 where we adapt attention knock-out to Mamba.

B Challenges in Performing Attention Knock-out in Mamba

Attention heads in autoregressive transformer LMs and Conv + SSM operations in Mamba play a similar role: bringing/retaining information from the past tokens. Attention *"knock-out"* is a type of causal mediation analysis that tries to understand information flow in transformer LMs by cutting off information propagation from k^{th} token to q^{th} token position. In transformers, each of the attention heads in an attention module $attn^{(\ell)}$ calculates an *attention matrix* L, where $\mathrm{L}_{q,k}$ quantifies how much attention is being paid to the k^{th} token by the q^{th} token with this specific attention head (see Vaswani et al. (2017) for details on the attention operation). We can block the information flow from k^{th} token to q^{th} token via a specific attention head by simply setting $\mathrm{L}_{q,k} := -\infty$ in the forward pass.

For Mamba, Ali et al. (2024) show that the amount of information retained in the q^{th} token state $s_q^{(\ell)}$, from the *convolved* state at k^{th} token $c_k^{(\ell)}$ (where $k < q$), after the selective-SSM operation (see Equations 4 and 5) can be visualized as an *attention matrix* per channel. Since the selective-SSM operation is linear, the information retained in $s_q^{(\ell)}$ from $c_k^{(\ell)}$ can

[3] www.wikidata.org/wiki/Wikidata:Main_Page

be calculated accurately as $\tilde{\alpha}_{q,k}^{(\ell)} = \overline{\mathrm{C}}_q^{(\ell)} \left(\prod_{i=k+1}^{q} \overline{\mathrm{A}}_i^{(\ell)} \right) \overline{\mathrm{B}}_k^{(\ell)} c_k^{(\ell)}$, where $\overline{\mathrm{A}}_i^{(\ell)}$, $\overline{\mathrm{B}}_i^{(\ell)}$, and $\overline{\mathrm{C}}_i^{(\ell)}$ are input-dependent parameters for the i^{th} token. See Gu & Dao (2023) and Ali et al. (2024) for details on selective-SSM operation. We ask: can we block the information flow from the k^{th} token to the q^{th} token in Mamba by subtracting out $\tilde{\alpha}_{q,k}^{(\ell)}$ from $s_q^{(\ell)}$? If so, attention knockout experiments in Mamba become feasible.

We find that blocking information flow via Conv + SSM operation through this specific edge from the k^{th} token to the q^{th} token can be challenging in Mamba. Note that, since $c_k^{(\ell)}$ is a *convolved* state with a receptive field of size 4 in Mamba-2.8b, the states $c_{k+1}^{(\ell)}$, $c_{k+2}^{(\ell)}$, and $c_{k+3}^{(\ell)}$ also retain information from $a_k^{(\ell)}$. Which means that even if we subtract $\tilde{\alpha}_{q,k}^{(\ell)}$ from $s_q^{(\ell)}$, these states can *"leak"* information about $a_k^{(\ell)}$ to $s_q^{(\ell)}$. To stop this leakage, we would want to subtract from $s_q^{(\ell)}$ all the information retained from $a_k^{(\ell)}$ via $c_{k+1}^{(\ell)}$, $c_{k+2}^{(\ell)}$, and $c_{k+3}^{(\ell)}$ states as well. However, accurately calculating this is challenging because of the SiLU non-linearity after Conv1D (see Equation (4)).

In our initial experiments we tested subtracting only $\tilde{\alpha}_{q,k}^{(\ell)}$ from $s_q^{(\ell)}$. But we found that Mamba-2.8b could often refer to the k^{th} token from the q^{th} token in copy and factual recall tasks.

C Isolating The Contribution of $\mathrm{W}_o^{(\ell)}$

Recall from Figure 1 and Equation (2) that when $o_i^{(\ell)}$ is restored, the $s_i^{(\ell)}$ and $g_i^{(\ell)}$ are restored as well. To isolate the contribution of only $\mathrm{W}_o^{(\ell)}$ we subtract out $\mathrm{IE}_{s_i^{(\ell)}} + \mathrm{IE}_{g_i^{(\ell)}}$ from $\mathrm{IE}_{o_i^{(\ell)}}$ and plot the results on Figure 8. Notice that subtracting $\mathrm{IE}_{s_i^{(\ell)}}$ cancels out the high indirect effect at the late site shown by later layers at the last token position. But, together $\mathrm{IE}_{s_i^{(\ell)}} + \mathrm{IE}_{g_i^{(\ell)}}$ cannot cancel out high $\mathrm{IE}_{o_i^{(\ell)}}$ observed at the early site, that is early-mid layers at the last subject token. This reconfirms the mediating role of $\mathrm{W}_o^{(\ell)}$ at the early site while recalling a fact.

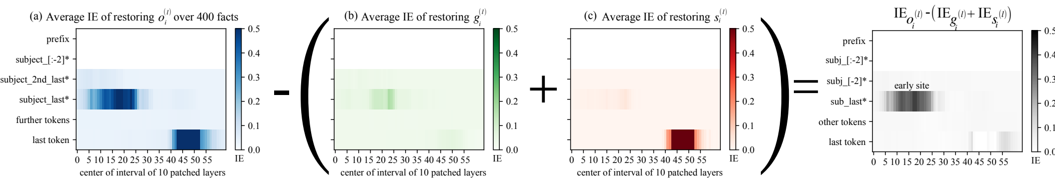

Figure 8: Isolating the contribution of $\mathrm{W}_o^{(\ell)}$. $\mathrm{IE}_{s_i^{(\ell)}} + \mathrm{IE}_{g_i^{(\ell)}}$ subtracted from $\mathrm{IE}_{o_i^{(\ell)}}$. Notice that $\mathrm{IE}_{o_i^{(\ell)}} - \left(\mathrm{IE}_{s_i^{(\ell)}} + \mathrm{IE}_{g_i^{(\ell)}}\right)$ still shows higher causal effect at the early site (more pronounced than $\mathrm{IE}_{g_i^{(\ell)}}$) while the high causal effect at the late site cancels out.

D Locating Key Modules in Pythia-2.8b

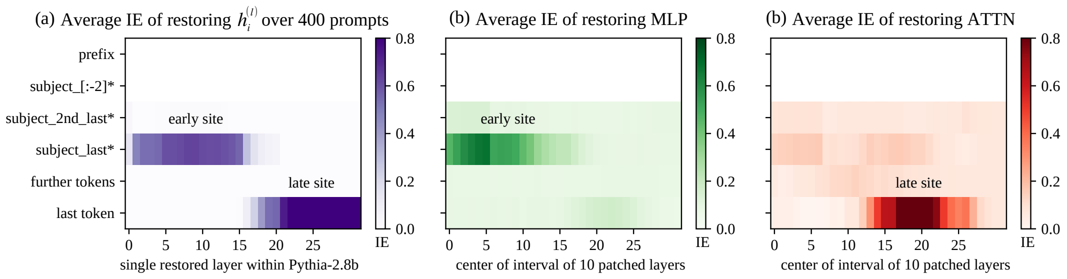

Figure 9: Average indirect effect of residual state, MLP, and attention outputs in Pythia-2.8b over 400 facts. For MLP and attention outputs a window of 10 layers around ℓ is restored, as restoring just one layer barely shows visible patterns.

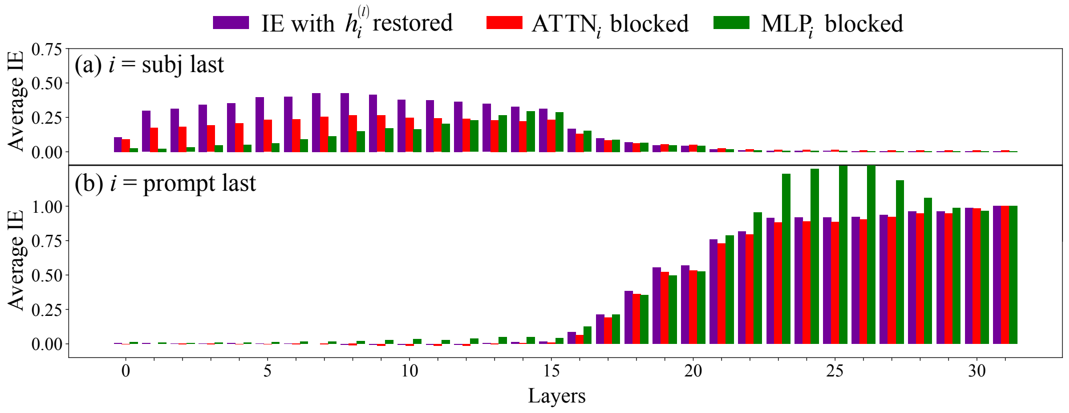

Figure 10: Impact of ablating ATTN$_i$ or MLP$_i$ on IE$_{h_i^{(\ell)}}$ for **(a)** *subject last* and **(b)** *prompt last* token positions on Pythia-2.8b

E Linearity of Relation Embedding (LRE)

With activation patching we can identify *where* facts are located inside a LM. We are also interested in understanding *how* LMs extract this information given $x = (s, r)$. Figures 2b and 5 show a clear separation of roles in early-mid and later layers in Mamba. We observe a similar phenomenon in autoregressive transformer LMs (Meng et al., 2022a;b; Geva et al., 2023). According to Geva et al. (2023), in transformer LMs, the subject entity representation $\mathbf{s}$, at the subject last token position, goes through an *enrichment* process, mediated by the MLP in the early-mid layers, where $\mathbf{s}$ is populated with different facts/attributes relevant to the subject entity s. Then, at the last token position, attention modules perform a *query* on the *enriched* $\mathbf{s}$ to extract the answer to the prompt $x = (s, r)$. Hernandez et al. (2023) approximate the *query* operation performed on the *enriched* $\mathbf{s}$ for a specific relation r by taking the first order Taylor series approximation (LRE) of the LM computation F as

$$F(\mathbf{s}, r) \approx \beta\, \mathrm{J}_\rho \mathbf{s} + b$$
$$\text{where } \mathrm{J} = \mathbb{E}_{\mathbf{s}_i, r}\left[\frac{\partial F}{\partial \mathbf{s}}\bigg|_{(\mathbf{s}_i, r)} \right], \quad b = \mathbb{E}_{\mathbf{s}_i, r}\left[F(\mathbf{s}, r) - \frac{\partial F}{\partial \mathbf{s}}\, \mathbf{s}\bigg|_{(\mathbf{s}_i, r)} \right], \tag{8}$$
$$\beta \text{ is a scalar , and } \quad \rho \text{ is the rank of J}$$

Hernandez et al. (2023) show that for a range of different relations it is possible to achieve a LRE that is faithful to the model computation F by averaging the approximations of J and b calculated on just $n = 5$ examples. We utilize LRE to understand the complexity of decoding *factual* relations in Mamba. We find the hyperparameters β, ρ and the layer ℓ (where to extract the enriched $\mathbf{s}$ from) using grid search. For mathematical and implementation details, see Hernandez et al. (2023).

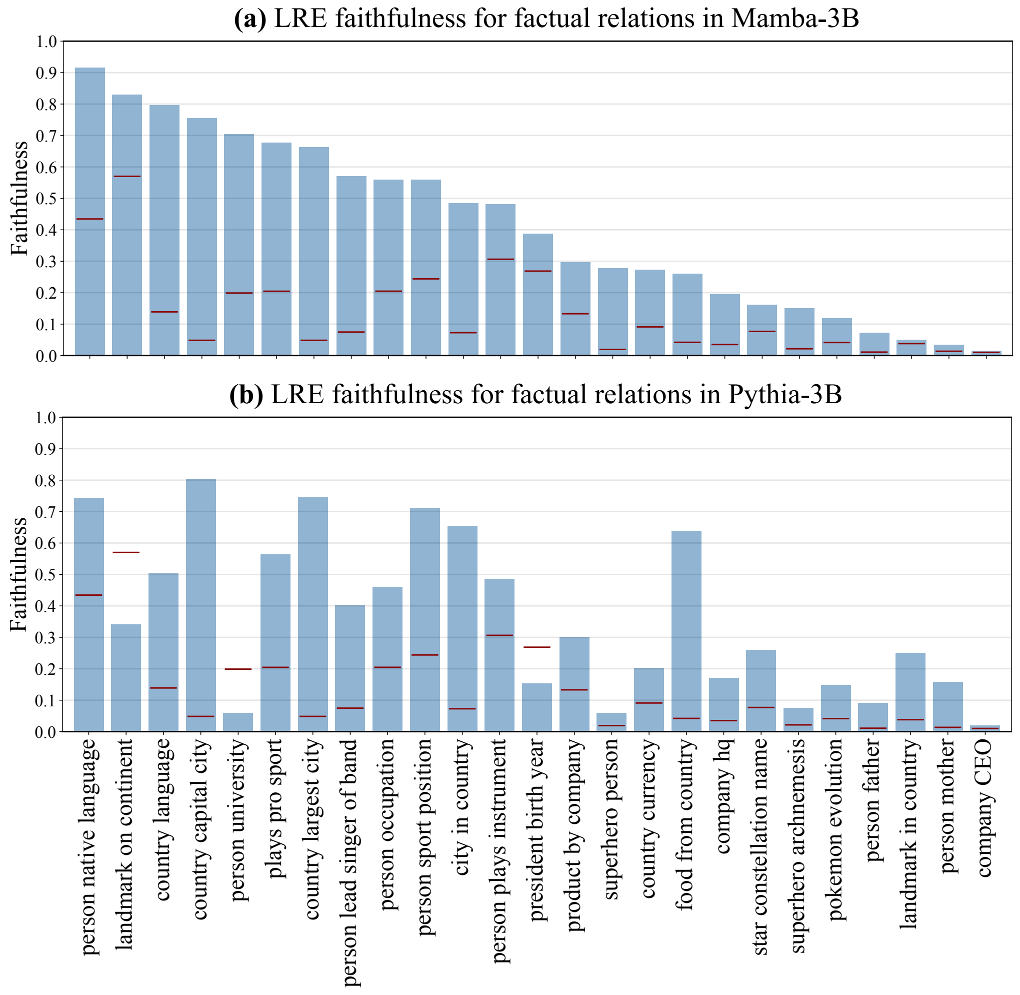

Figure 11: Relation-wise LRE *faithfulness* to the LM decoding function F for **(a)** Mamba-2.8b and **(b)** Pythia-2.8b. The relations are sorted according to their LRE faithfulness in Mamba-2.8b. Horizontal red lines per relation indicate random-choice baseline. We only present results for the *factual* relations in the RELATIONS dataset.

We plot the *faithfulness* of LRE with $n = 5$ samples on Figure 11 for Mamba-2.8b and similar sized Pythia. The metric *faithfulness* represents the portion of facts (s, r, o) that can be correctly retrieved if the LM computation $F(\mathbf{s}, r)$ is replaced with LRE$(\mathbf{s})$, a simple affine transformation.

We only calculate LRE for the *factual* relations in the RELATIONS dataset. Figure 11a shows that only for 10 out of 26 factual relations can a *linear* LRE achieve more than 50% *faithfulness*. For comparison, in the same sized Pythia-2.8b LRE achives $> 50\%$ *faithfulness* for 11 factual relations (see Figure 11b). And, in both Mamba and Pythia, LRE fails to achieve good *faithfulness* for the relations where the *range* (the number of unique answers) is large. These findings align with what Hernandez et al. (2023) observed on GPT and LLaMA models; suggesting that, similar to transformer LMs, factual knowledge might be heterogeneously represented for different relations in Mamba.

E.1 LRE Performance Across Different Layers

Besides *faithfulness* Hernandez et al. (2023) introduced another metric *causality* to measure the performance of LRE. Since LRE is a linear function, it is invertible. Assume that for a fact (s, r, o) LRE can faithfully replace LM computation $F(\mathbf{s}, r)$. Then given the representation $\mathbf{o}^*$ of another object o, $\text{J}^{-1}(\mathbf{o}^* - \mathbf{o})$ should give us a $\Delta\mathbf{s}$, such that when added to $\mathbf{s}$, $\tilde{\mathbf{s}} := \mathbf{s} + \Delta\mathbf{s}$, the model computation $F(\tilde{\mathbf{s}}, r)$ should generate o^*. See Hernandez et al. (2023) for details on this.

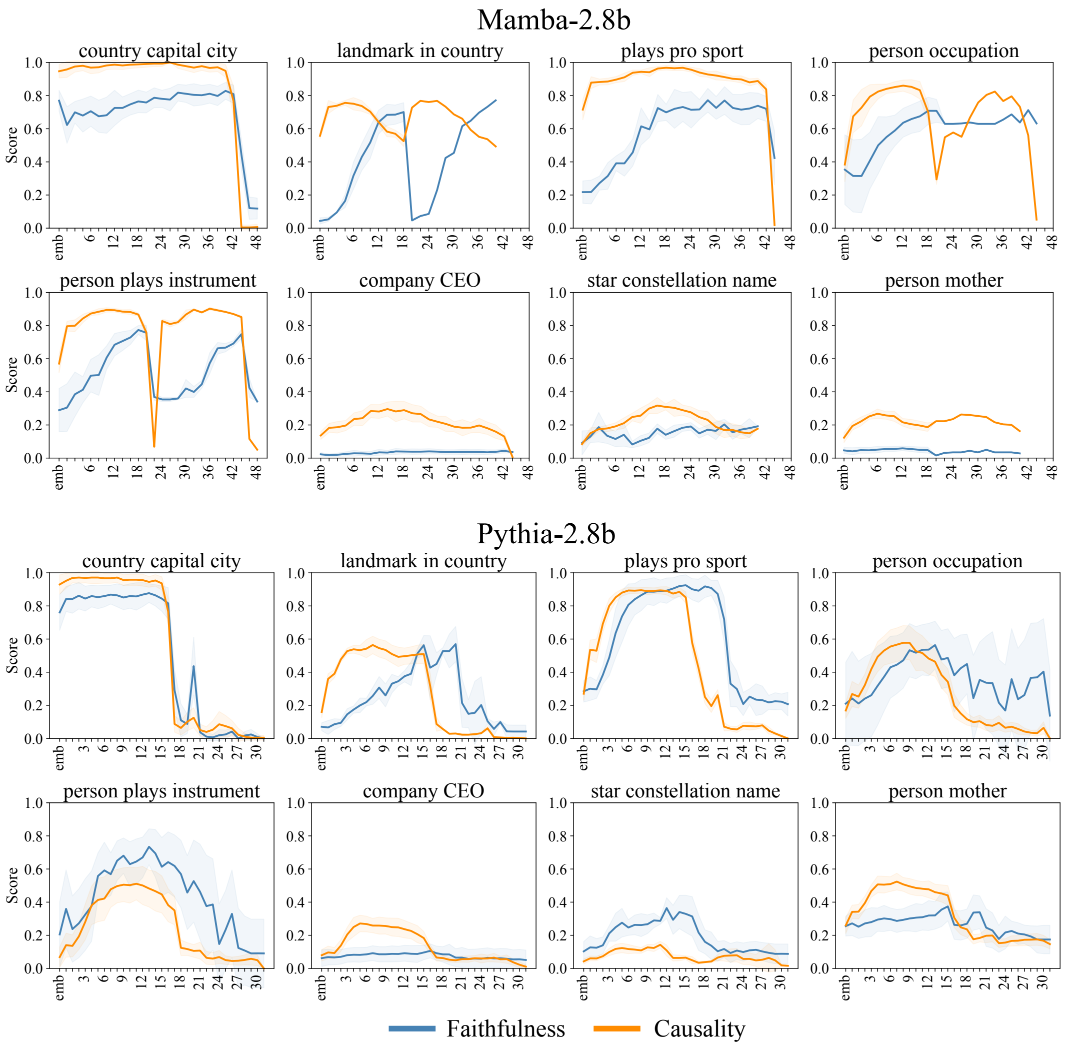

Figure 12: For Mamba, we only perform sweep till layer 48, as Figure 5 suggests negligible activity for later layers at the subject last token

F Activation Patching results on Mamba-2.8b

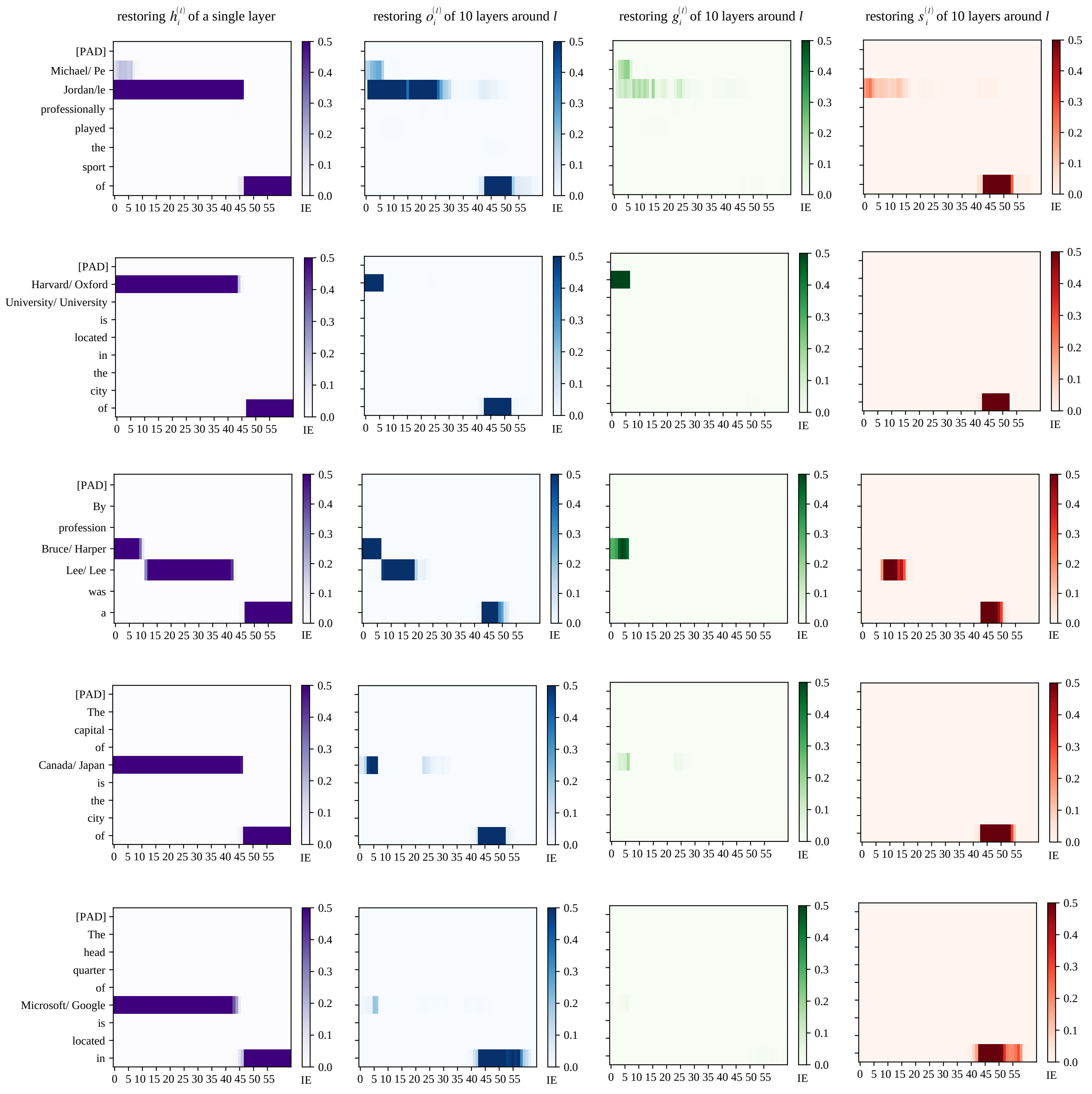
restoring $h_i^{(l)}$ of a single layer
restoring $o_i^{(l)}$ of 10 layers around l
restoring $g_i^{(l)}$ of 10 layers around l
restoring $s_i^{(l)}$ of 10 layers around l
[PAD]
Michael/ Pe
Jordan/le
professionally
played
the
sport
of
[PAD]
Harvard/ Oxford
University/ University
is
located
in
the
city
of
[PAD]
By
profession
Bruce/ Harper
Lee/ Lee
was
a
[PAD]
The
capital
of
Canada/ Japan
is
the
city
of
[PAD]
The
head
quarter
of
Microsoft/ Google
is
located
in
IE